Indian Journal of Engineering & Materials Sciences
Vol. 29, April 2022, pp. 169-180

# Effectively polymer composition controllable optical properties of PVDF/PMMA blend films for advances in flexible device technologies

Naresh Kumar, R J Sengwa*, Priyanka Dhatarwal, & Mukul Saraswat
Dielectric Research Laboratory, Department of Physics, Jai Narain Vyas University, Jodhpur 342 005, India

*Received: 28 December, 2021; Accepted: 21 March, 2022*

Polymer blends and their matrices-based nanocomposites have been established as potential candidates in the advancement of optoelectronic and microelectronic device technologies because they bear attractive design flexibility and also tunable optical and dielectric properties. In this research, we prepared the poly(vinylidene fluoride)/poly(methyl methacrylate) (PVDF/PMMA) blend films with varying constituents concentration (viz. PVDF/PMMA=100/0, 80/20, 60/40, 40/60, 20/80, 0/100 wt/wt%), and these were investigated by employing ultraviolet-visible (UV-Vis) spectrophotometer for their in-detail optical characterization. The absorbance, reflectance, and transmittance spectra of these PVDF/PMMA blend films in the wavelength range from 200 nm to 800 nm were analyzed and considered to determine the values of various optical parameters. Due to significant differences in optical behaviour of the PVDF film and that of the PMMA film, the values of the direct energy band gap, extinction coefficient, refractive index, single oscillator energy, dispersive energy, optical range complex dielectric permittivity, optical conductivity, linear susceptibility, third-order non-linear susceptibility, and non-linear refractive index of the PVDF/PMMA blend films were found appreciably blend composition controllable. The energy bandgap, refractive index, and extinction coefficient of these materials are found in the ranges 5.42 to 4.93 eV, 2.22 to 1.72, and $6.62 \times 10^{-4}$ to $0.64 \times 10^{-4}$, respectively. The experimental results offer a new paradigm for the use of these materials in the design and development of next-generation flexible optoelectronic and allied devices.

**Keywords:** Polymers, PVDF/PMMA blend, UV-Vis spectroscopy, Energy band gap, Optical properties

## 1 Introduction

In recent years, extensive efforts have been made to characterize various useful properties of the Polymer Blends (PBs) and the PBs matrices-based Polymer Nano Composites (PNCs) with the aims to explore their tunable character of optical, dielectric, as well as thermo-mechanical parameters that could help in the design guidelines for the creation of advanced electronic and optoelectronic devices[1–7]. Among the various PBs, the PVDF/PMMA blend is established as one of the superior properties polymer matrix to use directly or with some required additives for the advances in flexible device technologies including the sensors and energy generators[1–3,6–8]. Furthermore, among these polymers, the PMMA film has been recognized as a plexiglass material and its matrix-based PNCs have huge optoelectronic applications but its drawback is high brittleness with full bending and under stress[2,8,9]. To overcome this drawback, the PMMA blend with PVDF has been considered as an appropriate flexible type material[1–3,6–8,10]. The blending of PVDF reduces the brittleness of the PMMA structure due to the plasticizer behaviour of the PVDF[3,7,8,10]. The miscibility and processability of PVDF and PMMA blend materials have been explored by numerous researchers with the consideration of their optical transparency, solubility parameters, Flory-Huggins interaction parameters, thermal properties, and rheometry[1–3,10]. Most of these results evidenced that the dipole-dipole interaction of the hydrogen and fluorine atoms of the PVDF chain with the oxygen atoms of the carbonyl groups in the PMMA chain is predominantly responsible for large scale heterogeneous macromolecular compatibility and high miscibility of these polymers in the PVDF/PMMA blends.

The PVDF matrix is a semicrystalline fluoropolymer polymerized with $H_2C{=}CF_2$ monomer units, and it bears tremendous technologically driven promising properties like good mechanical, appropriate thermal, high dielectric, attractive piezoelectric as well as pyroelectric, high plasticity, and enough chemical and UV resistance[11–15]. Additionally, the degree of crystallinity of the PVDF film varies in a wide range depending on the PVDF polymerization process, the film preparation method,

*Corresponding author (E-mail: rjsengwa@rediffmail.com)

and various thermal, mechanical and electrical treatments of the prepared film[11,13,15]. The PVDF chain structures could crystallize in five distinct crystalline phases designated by α, β, γ, δ, and ε, and among these the polar β-phase is most important from the dielectric and energy applications point of view[8,11,13,14,15]. The non-polar α-phase with Trans-Gauche-Trans-Gauche (TGTG) conformation is easily formed by the melt crystallization process. However, the electro-active β-phase having planar zigzag conformation (TTTT) with all the fluorine atoms on one side and hydrogen atoms on another side of the PVDF chains can be achieved in appropriate amount through poling under a high electric field, mechanical deformation, and re-crystallization by melting under high pressure[11,15].

The PMMA matrix is a low-cost amorphous material, and its solution cast film has several excellent properties like high optical clarity, low refractive index, lightweight, high mechanical strength, good environmental inertness, and attractive dimensional and thermal stabilities[9,16–19]. The amorphicity of the PMMA matrix is due to the presence of bulky ester functional group ($O=C-O-CH_3$) as a pendant in its chain backbone[9,16]. It is a promising polymer matrix and frequently used for the development of a wide range of superior properties materials usable for sensors, solar cells, optical switches, optical fiber, transparent neutron stoppers, and radar wave magnifiers[9,16–21].

To integrate the attractive properties of both the PVDF and PMMA, a straightforward green chemistry approach is commonly used for making the films by blending these polymers in different compositions and also sometimes with important additives. These materials are characterized by employing various advanced techniques to explore technological usable properties and their dependence on the blend composition[1–3,6–8,10,22–26]. Our survey of the literature reveals that there is yet to investigate detail optical properties of the PVDF/PMMA blend films of varying composition. In this direction, the present study concerns the preparation of PVDF/PMMA blend films of entire range compositions by solution casting method. The detailed optical characterization of these films was performed to explore the composition tunable optical parameters and identify the potential applications in the development of flexible optoelectronic and microelectronic devices. These PVDF/PMMA films are characterized by a UV-Vis spectrophotometer for the absorbance $A$, transmittance $T$, and reflectance $R$ behaviour to the electromagnetic radiations of the wavelength range from 200 nm to 800 nm. Further analysis is made to determine direct band gap energy $E_{gd}$, extinction coefficient $k$, refractive index $n$, optical region complex dielectric permittivity ($\varepsilon'$, $\varepsilon''$), optical conductivity $\sigma_{opt}$, optical dispersion parameters, and non-linear optical parameters, and also to confirm the dependency of these parameters on the composition of the constituents of the polymer blend films.

## 2 Materials and Methods

### 2.1 Materials

Powder samples of the PVDF (average molecular weight $M_w$ ~ 534,000 g $mol^{-1}$) and the PMMA (average molecular weight $M_w$ ~ 350,000 g $mol^{-1}$) were obtained from Sigma-Aldrich Pvt. Ltd., France, and Sigma Aldrich Pvt. Ltd., Germany, respectively. The N,N-dimethyl formamide (DMF) for HPLC and UV spectroscopy grade was purchased from Loba Chemie Pvt. Ltd., India, and used as a common solvent for the PVDF and PMMA.

#### *2.1.1 Preparation of polymer blend films*

The PVDF/PMMA blend films with varying compositions (i.e., PVDF/PMMA=100/0, 80/20, 60/40, 40/60, 20/80, 0/100 wt/wt%) were prepared by solution casting film preparation method. The required amounts of these polymers, in weight, corresponding to a fixed blend composition were dissolved together in the DMF solvent at 60 $^oC$. A homogeneous solution was obtained in a stoppered conical glass flask with continuous magnetic bar stirring. Then, the polymeric solution was cast onto a glass Petri dish of diameter 4 cm and it was placed on a hot plate, thermostated at ~70 $^oC$, to evaporate the DMF solvent for achieving the material in film form. All the different composition PVDF/PMMA blend films were prepared by following the above said steps, and then these films were vacuum dried overnight at 45 $^oC$ to eliminate the solvent traces. The thicknesses $t$ of these PVDF/PMMA films are reported in Table 1. The digital picture of the PVDF/PMMA blend films with varying polymer compositions is shown in Fig. 1. One can see that the PVDF film is light yellowish-brown and has relatively low transparency. As the PVDF amount reduces and simultaneously the PMMA amount increases in the blends, the yellowish-brown colour of the films

Table 1 — Values of films thicknesses $t$, and their absorbance $A$, transmittance $T$, reflectance $R$, extinction coefficient $k$, refractive index $n$ (at $\lambda = 700$ nm), maximum optical conductivity $\sigma_{opt}$, and direct energy band gap $E_{gd}$ of the different composition PVDF/PMMA blend films

| PVDF/PMMA films (wt/wt%) | $t$ (mm) | $A$ | $T$ (%) | $R$ | $k \times 10^4$ | $n$ | $\sigma_{opt} \times 10^{-13}$ ($s^{-1}$) | $E_{gd}$ (eV) |
|---|---|---|---|---|---|---|---|---|
| 100/0 | 0.11 | 0.56 | 27.0 | 0.76 | 6.62 | 2.22 | 5.4 | 5.42 |
| 80/20 | 0.13 | 0.10 | 77.7 | 0.56 | 1.07 | 1.79 | 4.2 | 5.12 |
| 60/40 | 0.12 | 0.16 | 67.8 | 0.59 | 1.80 | 1.85 | 4.7 | 5.06 |
| 40/60 | 0.17 | 0.19 | 64.3 | 0.61 | 1.44 | 1.87 | 3.3 | 4.98 |
| 20/80 | 0.21 | 0.32 | 47.4 | 0.67 | 1.98 | 2.01 | 2.8 | 4.93 |
| 0/100 | 0.10 | 0.05 | 89.0 | 0.53 | 0.64 | 1.72 | 5.2 | 5.01 |

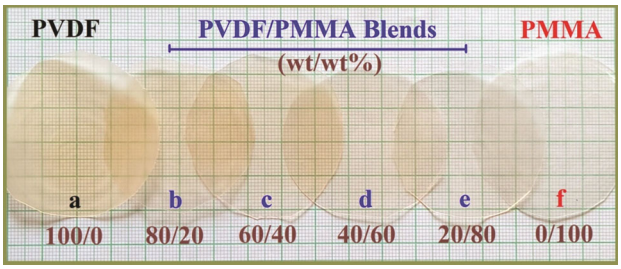


Fig. 1 — Digital pictures of different compositions PVDF/PMMA (a) - 100/0, (b) - 80/20, (c) - 60/40, (d) - 40/60, (e) - 20/80, and (f) - 0/100 wt/wt%) blend films.

diminishes and the transparency increases. Among these films, pure PMMA film has relatively higher transparency. Furthermore, the manual tests like twisting, bending, and touching realize that all these polymer films are reasonably flexible, non-sticky, and of smooth surfaces. The PMMA film shows likely brittle character when it is fully bent or twisted.

#### *2.1.2 Measurements*

The UV-Vis range absorbance of the electromagnetic radiations for each film was conducted with a UV-Vis spectrophotometer (Cary-60 of Agilent Technologies Pvt. Ltd.) at ambient temperature. The spectrometer used has double beam geometry and wavelength λ accuracy of 1 nm which is fully computer-controlled by Cary WinUV software. The absorbance spectra of the PVDF/PMMA films were measured by mounting each film in a solid sample holder with keeping the film surfaces exactly perpendicular to the incident photons of λ values in the range from 200 nm–800 nm. The measurements were performed at a sweep rate of 10 nm/s with the consideration of baseline corrections.

## 3 Results and Discussion

### 3.1. Absorbance spectra

Figure 2 presents the absorbance $A$, transmittance $T$(%), reflectance $R$, and absorbance coefficient α spectra of the PVDF/PMMA blend films having different compositions of their constituents. The electronic transitions in various orbitals are designated as σ, π, n, $\pi^*$, and $\sigma^*$, and some of these orbital transitions are accounts for the UV-Vis range wavelength-dependent absorbance of electromagnetic (EM) radiations in the polymers and their matrices based composite materials[4–6,15–19,27–42]. A relative analysis of the absorbance spectra of PVDF/PMMA films (Fig. 2(a)) explains that the pristine PVDF film has mild absorbance for the visible range photons confirming its little opaque character whereas the optical range absorbance by the pristine PMMA film is insignificant confirming its high optical transparency which is in agreement with the previous studies on these pristine polymer films [6,8,12,16,18,19,32,33,37,38]. In the UV region, these polymers films, firstly show a slow non-linear increase in absorbance with the decrease in λ value, and finally exhibited an abrupt huge increase below 250 nm which signifies some characteristic electronic transitions through the high energy bandgap. The electronic transitions ($\pi \rightarrow \pi^*$ and $n \rightarrow \pi^*$) from the carbonyl group (C═O) of monomer in the PMMA chain and the difluoromethylene group ($-CF_2$) in the repeat unit of PVDF chain are responsible for the observed strong lower UV wavelength range absorbance band in these polymeric materials[12,16,17,22]. The absorbance by the PVDF/PMMA blend films for visible range photons increased as the amount of PMMA was raised from 20 wt% to 80 wt%, which is the opposite behaviour of the expected trend from the absorbance of the pristine PVDF and PMMA films. This result may be due to some characteristic heterogeneous interactions between the hydrogen and/or fluorine atoms of the PVDF structure and the oxygen atoms of the PMMA structure which could also be the reason for the red shifting of the absorbance band edge from 252 nm to 258 nm as the PMMA amount increased in the PVDF/PMMA blend

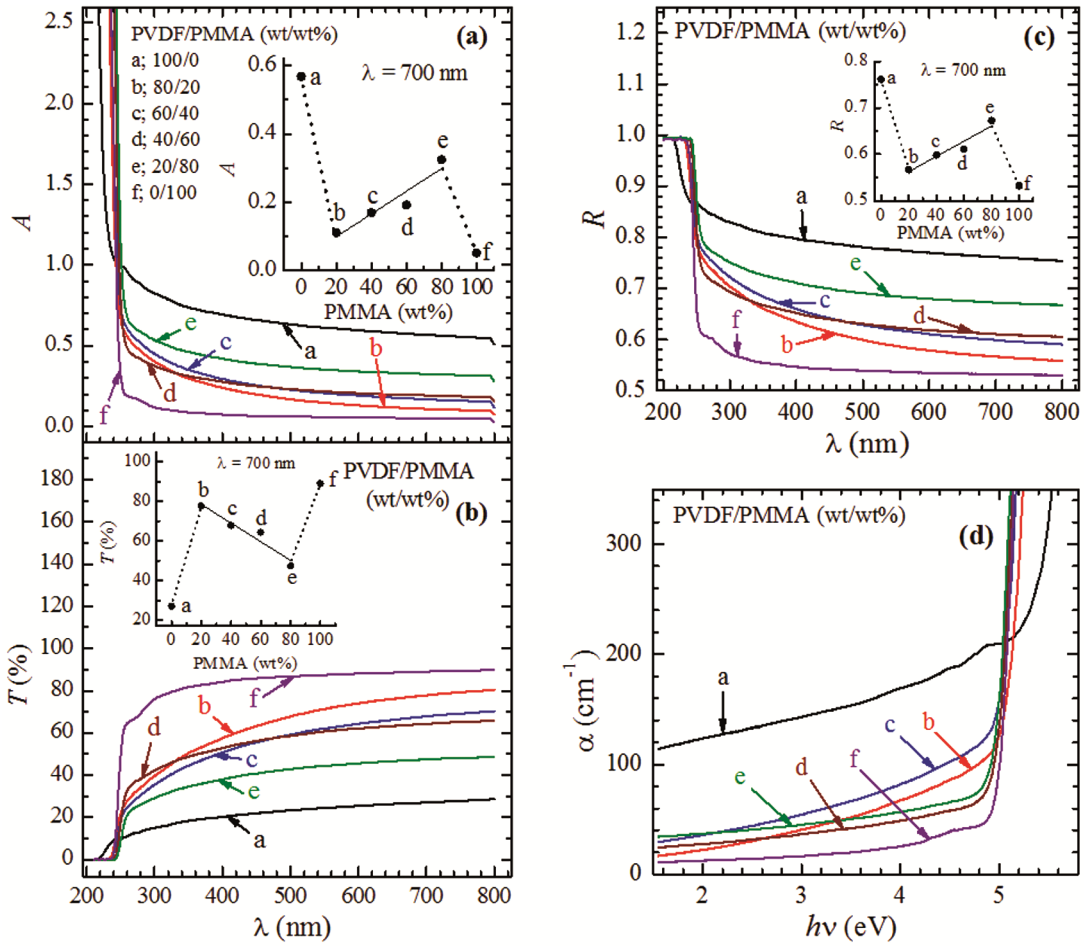


Fig. 2 — UV-Vis spectra (a) absorbance (*A*), (b) transmittance (*T*), (c) reflectance (*R*), and (d) absorption coefficient (α) versus photons energy (*hν*) for different compositions PVDF/PMMA (a - 100/0; b - 80/20; c - 60/40; d - 40/60; e - 20/80; f - 0/100 wt/wt%) blend films at ambient temperature. Insets show the variation of *A*, *T*, and *R* (at λ = 700 nm) with PMMA wt% for these PVDF/PMMA blend films. Solid lines in insets represent the linear fit of data for the blend films.

films. The inset plot of Fig. 2(a) illustrates the variation of absorbance *A* with increasing PMMA concentration in the PVDF/PMMA blend films, at a fixed λ of 700 nm, and these *A* values are also listed in Table 1. This inset plot clarifies that the absorption for the photons of the visible region can be regulated appreciably by altering the compositional ratio of the constituents in the PVDF/PMMA blend films.

### 3.2. Transmittance spectra

The percent transmittance *T*(%) values of the PVDF/PMMA blend films in the UV-Vis wavelength range (200 nm – 800 nm) are determined from the respective wavelength λ absorbance *A* values by using the following relation[27,28,30,31] given in Eq. (1);

$$T(\%) = \text{Antilog}\,(2-A) \qquad \ldots (1)$$

For the PVDF/PMMA blend films, their *T*(%) versus λ plots are depicted in Fig. 2(b). The transmittance plots of the PVDF/PMMA blend films appeared inverted replicas of their absorbance plots, which is as expected from the *A* and *T* relation given in Eq. (1), and also found consistent with other polymeric materials[30,31]. Further, over the UV wavelength of the electronic transition band, the *T* values are zero for these films. Among these films, the pristine PVDF film can be identified with the lowest transmittance whereas the pristine PMMA film has relatively high transmittance in the wavelength region starting from 250 nm and extending up to 800 nm. Additionally, the transmittance values of the PVDF/PMMA blend films lie in between the transmittance range of the constituents polymers which is as expected by the simple blending rule. The inset figure of Fig. 2(b) confirms that the transmittance values, at the incident photon of 700 nm, for the PVDF/PMMA films (values of *T*

at this wavelength are also provided in Table 1) decreased with an increase of the PMMA amount in the blend films. These findings suggest the suitability of the PVDF/PMMA blend materials as visible range photons intensity attenuators/controllers where such materials are needed in the design of flexible optoelectronic devices and their use in UV radiation shielders. Furthermore, the transmittance values of PVDF/PMMA films abruptly decreased with the lowering of λ value below 250 nm which also identifies the electronic transitions. The electrons from the fluorine atoms and oxygen atoms of the functional groups of these polymers get active by absorbing the UV radiations of higher energy and jump to the conduction band by crossing the barrier height of energy bandgap $E_g$. But the photons of high wavelength in this experimental range do not have sufficient amount of energy needed to make the electrons free from bound orbit, and therefore, the incident electromagnetic radiation energy is not absorbed by the polymeric materials and most of that is directly transmitted which is reasonably demonstrated for such type of polymers in the previous literature[6,16,27,28,30,31,34].

### 3.3. Reflectance spectra

Reflectance $R$ values of the PVDF/PMMA blend films for the incident photons of varying wavelength λ were determined using their $A$ and $T$ values in the exponential relation[27,28] given in Eq. (2);

$$R = 1 - (T \times \exp A)^{1/2} \quad \text{... (2)}$$

The $R$ versus λ spectra of these PVDF/PMMA blend materials are shown in Fig. 2(c), which seem identical to the shape of their absorbance spectra with limiting to $R$=1 over the electronic transition band wavelength range. Comparatively, it is noted that the reflectance value for the pristine PMMA film is relatively low, and its value is high for the PVDF film in the visible range which also remained almost stable with λ variation from 800 nm to 400 nm. A step increase in the reflectance for the lower wavelength UV-radiation is a characteristic of these spectra which can be ascribed to the electronic transitions. The inset of Fig. 2(c) demonstrates that there is an increase of $R$ values, at a fixed wavelength λ=700 nm of incident photon on the PVDF/PMMA films when the PMMA amount is raised in the blends. The $R$ values at λ=700 nm are also listed in Table 1 for the interest of readers and the technical uses of these films. These PVDF/PMMA blend materials having an increasing trend of reflectance could be potential candidates for reflectance coatings in LASER technologies[17,32,33].

### 3.4. Absorption coefficient

The absorption coefficient α is a measure of material capacity to absorb the amount of incident radiation intensity per unit sample thickness $t$, and therefore its study is highly meaningful regarding the selection of an appropriate material for optoelectronic applications[16,19]. The Beer-Lambert law relates the α with $t$ of a film with the incident and transmittance photon intensities $I_o$ and $I$, respectively by the Eq. (3), and in the form of absorbance $A$ (i.e., log ($I_o$/$I$)) is given in Eq. (4), which are demonstrated in detail in the previous literature[17,27,28,30];

$$I = I_o e^{-\alpha t} \quad \text{... (3)}$$

$$\text{And, therefore } \alpha = \frac{2.303}{t} \log \frac{I_o}{I} = \frac{2.303 A}{t} \quad \text{... (4)}$$

Figure 2(d) shows the plots of α versus photon energy $h\nu$ for the PVDF/PMMA films. The α values for the pristine PMMA film and also the PVDF/PMMA blend films are found much lower than that of the pristine PVDF film. But these values for all the materials have a gradual increase with the increase of incident photons energy $h\nu$ ($h$ is the Planck's constant and ν is the frequency of photon), and lastly exhibited a steep rise when the $h\nu$ reached closer or equal to the required energy for electronic transitions of the valence band electrons. For these PVDF/PMMA materials, the electronic transition energy seems about 5 eV, from their α versus $h\nu$ plots.

### 3.5. Tauc plots and energy band gaps

Particular interest in the study of optical energy band gap $E_g$ of the polymers and polymeric composites is to identify their appropriateness in the design and development of different flexible type optoelectronic devices[4–6,12,16–19,28–33]. The direct and indirect electronic transitions in such optical materials obey the Davis and Mott's relation given in Eq. (5), and the detailed procedure for determination of energy band gap corresponding to these transitions has been described in some of the earlier researches[16,28,30,31,42];

$$(\alpha h\nu)^m = B(h\nu - E_g) \quad \text{... (5)}$$

Where, $B$ is proportionality constant and $m$ is a variable having values are 2 and 1/2 corresponding to the direct energy bandgap $E_{gd}$ and the indirect energy bandgap $E_{gi}$ of an optical material. To determine the

$E_{gd}$ values of the PVDF/PMMA films, their Tauc's plots ($(\alpha h\nu)^2$ versus $h\nu$) are depicted in Fig. 3(a). Applying extrapolation procedure on the linear part of absorption edge to the $x$-axis where the values of $(\alpha h\nu)^2$ turn zero, at that point the $h\nu$ value gives the $E_{gd}$ value, and the estimated $E_{gd}$ values by this procedure for the PVDF/PMMA films are listed in Table 1. The $E_{gd}$ values of the pristine PVDF film and the PMMA film are found to be 5.42 eV and 5.01 eV, respectively which are in close agreement with their literature values[12,16]. The $E_{gd}$ values of the PVDF/PMMA blend films decreased linearly with the increasing amount of PMMA in these polymer blend films which can be seen from Fig. 3(b). This behaviour is corroborated with the electronic structural disordering (some displacement in atoms positions and also the changes related to electronic charge distribution) in the blended polymers and also with the change of their amounts in the blend. Such disordering causes the formation of some localized energy density states in the potential barrier height (i.e., the forbidden energy band gap) and these states are mostly exhibited just above the valence band and below the starting of the conduction band edge as defined earlier[4,5,16,27,30,39]. The linear variation of $E_{gd}$ values with the alteration of constituents polymer amount in the PVDF/PMMA blend films evidence that these easily twistable and bendable blends could be used as energy bandgap tuner materials in the design of some advanced flexible type optoelectronic devices. The tunable band gap values with the blend composition are also reported for some other blends of polymers[38].

### 3.6. Refractive index and extinction coefficient

The linear refractive index $n$ is one of the most significant optical parameters which explains the propagation behaviour of the photon energy through an optical material. Additionally, it is applied in the determination of several other optical properties like optical range dielectric permittivity, electrical conductivity, and the dispersion parameters (viz. oscillator energy $E_o$, dispersive energy $E_d$, and static refractive index $n_o$)[28–31].

The complex refractive index $n^*$ as a function of photons wavelength λ for an optical material is described by Eq. (6),[30,31]

$$n^*(\lambda) = n(\lambda) + ik(\lambda) \quad \ldots (6)$$

where, the real and imaginary parts of the $n^*(\lambda)$ are called linear refractive index $n(\lambda)$ and extinction coefficient $k(\lambda)$, respectively for an optical material. The $n(\lambda)$ values of an optical material can be determined from the λ dependent $R$ values using the relation[27,28,30] given in Eq. (7),

$$n(\lambda) = \frac{1+R^{1/2}}{1-R^{1/2}} \quad \ldots (7)$$

The $n$ versus λ plots for the PVDF/PMMA blend films are presented in Fig. 4(a) which exhibited the same type of shapes as that of the $R$ versus λ plots (Fig. 2(c)). Initially, the $n$ values of the PVDF/PMMA films are about 3 over the wavelength range of absorbance band which abruptly drops at UV-radiation wavelength where the electronic transitions initially occurred, and thereafter it decreases a little with further increase of λ up to

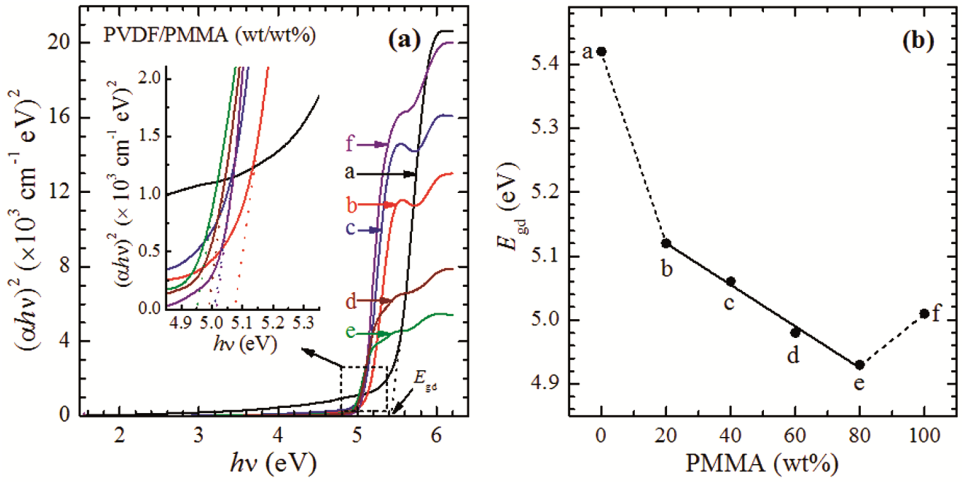


Fig. 3 — (a) Tauc's plots ($(\alpha h\nu)^2$ versus photon energy $h\nu$) for different compositions PVDF/PMMA (a - 100/0; b - 80/20; c - 60/40; d - 40/60; e - 20/80; f - 0/100 wt/wt%) blend films (inset shows enlarged view around the onset of steep rise), and (b) plot of direct energy band gap $E_{gd}$ versus PMMA (wt%) of the PVDF/PMMA blend films. The solid line in (b) represents the linear fit of data for the blend films.

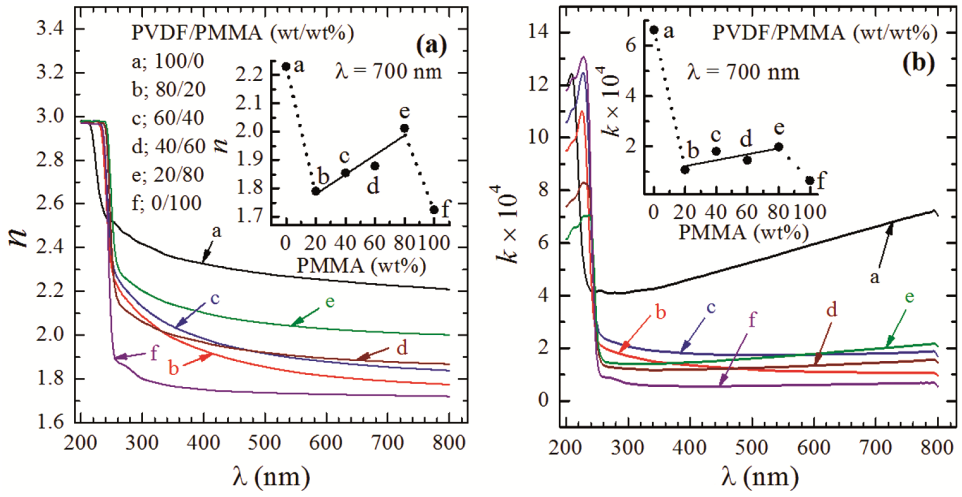


Fig. 4 — Plots of (a) refractive index $n$ and (b) extinction coefficient $k$ versus photons wavelength λ for the different compositions PVDF/PMMA (a - 100/0; b - 80/20; c - 60/40; d - 40/60; e - 20/80; f - 0/100 wt/wt%) blend films at ambient temperature. Insets present the $n$ and $k$ (at λ = 700 nm) versus PMMA (wt%) plots for these blend films. Solid lines in insets represent the linear fit of data.

800 nm. More correctly, the $n$ values are almost static over the entire visible range which infers the normal dispersion of light energy[28,30]. The $n$ values of the PVDF film over the entire wavelength range are relatively high as compared to the PMMA and the PVDF/PMMA blend films, and these values remain around 2.3 in the wavelength of the visible range, whereas for the PMMA film it is found about 1.75 (see Fig. 4(a)). A huge difference in the $n$ values of the PVDF film and the PMMA film confirms their different characteristic interactions with the propagating photons. The $n$ values of the PVDF/PMMA films lie between that of the pristine PVDF film and the PMMA film, and also showed a linear variation (at λ = 700 nm) with the change in their constituents composition which can be noted from the inset of Fig. 4(a). This finding explains that the PVDF/PMMA blend materials can be used to design a refractive index controllable optical device. Furthermore, the $n$ values of the PVDF/PMMA films at 700 nm are listed in Table 1 for the benefit of the readers and the end-users.

The $k(\lambda)$ value is a measure of energy loss of the propagating photon as a result of its interaction with the charge carriers like free electrons in the material. The $k$ of a material has a proportionality relation with the α and λ as defined by relation[28,30,31] given in Eq. (8);

$$k(\lambda) = \frac{\alpha\lambda}{4\pi} \quad \ldots (8)$$

It can be seen from Fig. 4(b) that the $k$ values of PVDF/PMMA blend films abruptly reduced at the onset wavelength of electronic transitions which occurs in the UV region. This abrupt changing edge also explains that the electrons got excited to a higher energy state because the incident photons have the energy either equal or higher than the energy bandgap. But as the energy of photons become slightly lower as compared to the forbidden energy bandgap of the material then their absorbance probability by the material is low. Therefore, the energy loss becomes minimum in the material, and as a result, the $k(\lambda)$ values appeared relatively very low in the visible region[30]. Further, the observed low losses of photons energy in the entire visible region are due to a reflection and/or scattering phenomena exhibited by the PVDF/PMMA blend films[28–32]. Furthermore, after an abrupt drop, the $k(\lambda)$ value of pristine PVDF film linearly increased in the λ range from 260 nm to 800 nm which may be due to its ferroelectric characteristics[11,14]. A plot of $k$ (at 700 nm) versus PMMA concentration for these PVDF/PMMA films is shown in the inset of Fig. 4(b) which explains that there is an anomalous increase in $k$ values but these values are close to that of the pristine PMMA film and much lower than the pristine PVDF film. The $n$ and $k$ values of the PVDF/PMMA films at 700 nm are also listed in Table 1. These results reveal that the PVDF/PMMA blends are attractive optical materials having low losses with tunable refractive index in the broader wavelength range, from 300 nm to 800 nm, which could be suitable for the advances in the fabrication of flexible optoelectronic components/devices.

### 3.7. Optical range dielectric permittivities and losses

The incident photons wavelength λ dependent complex dielectric permittivity ε* of the PVDF/PMMA films was determined from their *n* and *k* values using the relation[27,30,31] given in Eq. (9);

$$\varepsilon^*(\lambda) = \varepsilon'(\lambda) - i\varepsilon''(\lambda) = n^2 - k^2 - i2nk \quad \ldots (9)$$

Where the real part ε′(λ) represents the energy storage capacity of the material and the imaginary part ε″(λ) is a measure of energy losses for the photons. The plots of ε′ and ε″ versus *hν* for the PVDF/PMMA films are illustrated in Fig. 5(a and b), respectively. Figure 5(a) shows that the ε′ values of these polymer blend films have a gradual increase with the increase of photons energy from 1.55 eV to about 4.52 eV, and then sharply increased and attained a steady value of about 9 for the higher *hν* photons. Moreover, it is found that the ε′ values of pristine PMMA film are about 3 which remained almost steady for the photons of energy range from 1.55 eV to 4.0 eV (the λ range from 800 nm to 310 nm) which confirms it a low dielectric constant material for the entire visible range electromagnetic radiations. In contrast to the PMMA film, the ε′ values of the PVDF film are high and exhibited a gradual increase from ~ 5 to 6.4 with reducing λ values from 800 nm to 250 nm which identifies the PVDF as a relatively high dielectric constant polymer material. The ε′ values of the PVDF/PMMA blend films are found in between that of the PMMA film and the PVDF film, and also exhibited an anomalous increase with the increase of PMMA amount in the blend films which can be noted from the inset plot of ε′ versus PMMA (wt%) given in Fig. 5(a).

Figure 5(b) demonstrates that the ε″ values of pristine PVDF film decreases non-linearly from ~ 0.003 to 0.002 with increasing incident photon energy *hν* from 1.55 eV to about 5.04 eV, and thereafter the ε″ sharply increased to 0.0075. In contrast to the PVDF film, the PMMA film and also the PVDF/PMMA films have very low ε″ values for the photons of energy range from 1.55 eV to 4.85 eV and then increased abruptly at about 5 eV. The ε″ values of the PMMA film are about 0.0003 and the PVDF/PMMA blend films are lower than 0.001 which categories these materials as very low loss dielectrics for the visible range photons and also for higher wavelength UV-radiations. The interesting outcomes from the analysis of ε′ and ε″ values of these polymer materials are (i) the PMMA film is a low dielectric constant and insignificant dielectric loss optical material, (ii) PVDF film is a relatively higher dielectric constant and moderate loss optical material, and (iii) the PVDF/PMMA blend films confirm their suitability as moderate dielectric constant and mild dielectric loss material for the visible range electromagnetic radiations.

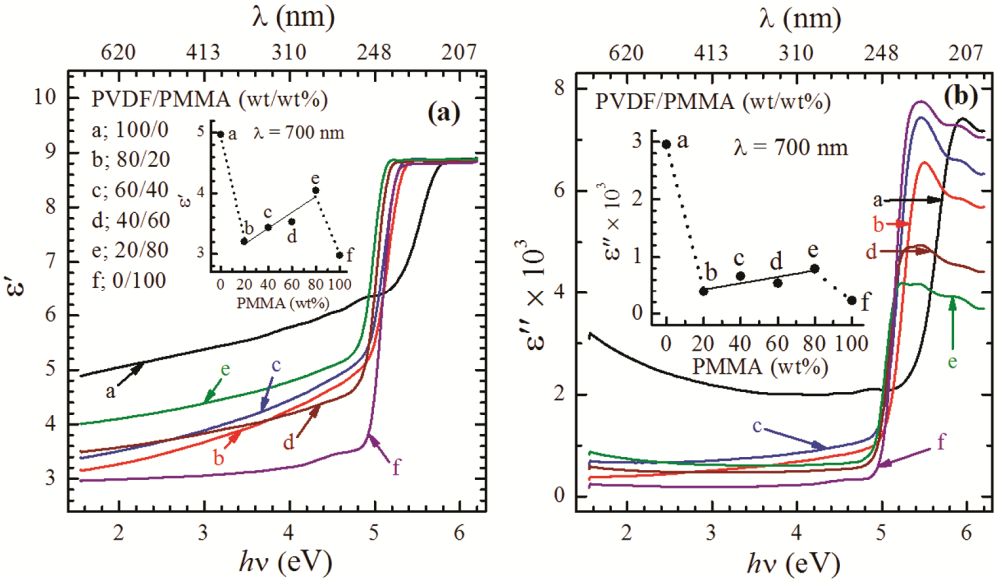


Fig. 5 — Plots of (a) optical dielectric constant ε′ and (b) dielectric loss ε″ versus incident photon energy *hν* (or wavelength λ) for the different compositions PVDF/PMMA (a - 100/0; b - 80/20; c - 60/40; d - 40/60; e - 20/80; f - 0/100 wt/wt%) blend films at ambient temperature. Insets depict the ε′ and ε″ (at λ = 700 nm) versus PMMA (wt%) plots for these blend films. Solid lines in insets represent the linear fit of data for the blend films.

### 3.8. Optical conductivity

The study of optical conductivity $\sigma_{opt}$ gives information about the existing electronic states in the optical material[27,30]. The proportionality relation[6,28,29,31] of $\sigma_{opt}$ with the absorption coefficient α and refractive index $n$, in the Gaussian system of units is given in Eq. (10),

$$\sigma_{opt} = \frac{\alpha n c}{4\pi} \quad \ldots (10)$$

where, $c$ is free space velocity of light ($c$ = 3 x $10^{10}$ cm/s). The values of $\sigma_{opt}$ for the PVDF/PMMA blend films corresponding to different energy photons are computed from Eq. (10) and these are plotted in Fig. 6. It can be seen from this figure that the $\sigma_{opt}$ values increased slowly with the increase of incident photons energy $h\nu$ over the visible region which is attributed to the diffusion of excess charge carriers that are released in an optical material when electronic structural disordering occurred as a result of photons interaction[28,29]. The maximum $\sigma_{opt}$ values of these materials corresponding to photons energy of 6 eV are listed in Table 1. It has been noted that the PVDF/PMMA blends have a small lowering in their maximum optical conductivity values as compared to the pristine PVDF and PMMA films. Furthermore, there is about one order of magnitude high $\sigma_{opt}$ value for the PVDF film as compared to the PMMA film at the photon energy of 2 eV, whereas the $\sigma_{opt}$ values of these polymer blend films are in between that of the values of the constituents which is interesting from their use as conductivity controllable optical materials.

### 3.9. Dispersive parameters

The optical dispersive parameters such as single oscillator energy $E_o$ (it represents an average energy band gap), dispersive energy $E_d$ (which is a measure of inter-band optical transitions), and the static refractive index $n_o$ of optical material can be computed using a single oscillator model derived by Wemple and DiDomenico (WDD)[43] (Eq. (11)) which has been recently applied on different polymeric materials[6,28,31,36,44];

$$(n^2-1)^{-1} = \frac{E_o}{E_d} - \frac{(h\nu)^2}{E_o E_d} \quad \ldots (11)$$

The linear refractive index $n$ in Eq. (11) is termed $n_o$ at $h\nu = 0$ which can be determined by Eq. (12);

$$n_o = \left(1 + \frac{E_d}{E_o}\right)^{1/2} \quad \ldots (12)$$

The WDD model explains that a plot is drawn between $(n^2-1)^{-1}$ and $(h\nu)^2$ for an optical material may exhibit a linear behaviour over the lower range values of $(h\nu)^2$. From such a linear plot, the $E_o$ and $E_d$ values can be estimated by taking the slope value (that gives the value of $E_o/E_d$) and the intercept value on the $(n^2-1)^{-1}$ axis (that is numerically equal to $1/E_oE_d$).

The $(n^2-1)^{-1}$ versus $(h\nu)^2$ plots for the PVDF/PMMA blend films of varying compositions are shown in Fig. 7, which exhibited a straight line

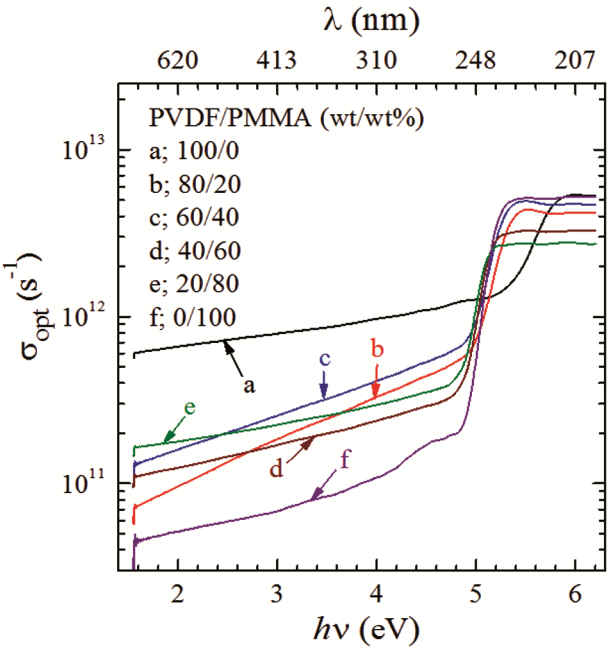


Fig. 6 — Plots of optical conductivity $\sigma_{opt}$ versus $h\nu$ (or λ) for the different compositions PVDF/PMMA blend films.

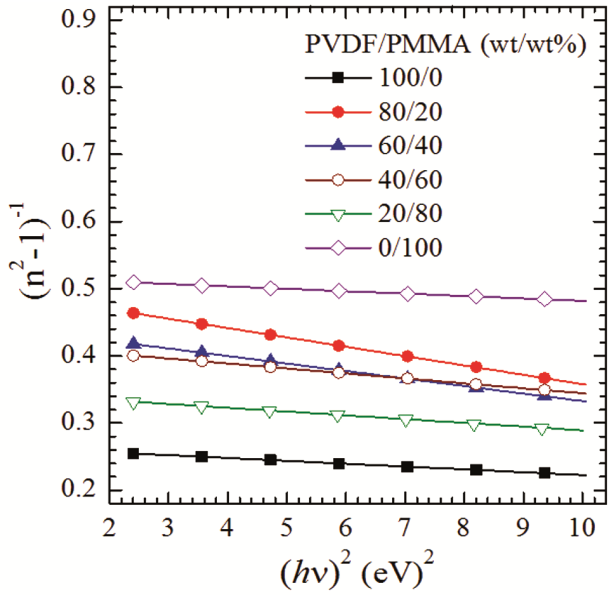


Fig. 7 — Plots of $(n^2-1)^{-1}$ versus $(h\nu)^2$ for different compositions PVDF/PMMA blend films.

behaviour. Therefore, by noting the slope and intercept values from these lines, the $E_o$ and $E_d$ values were determined and then the $n_o$ values were computed for the PVDF/PMMA films, and all these parameters values are listed in Table 2. Figure 8(a) demonstrates the variation of $E_o$, $E_d$, and $n_o$ values with the PMMA (wt%) amount for the PVDF/PMMA blend films. It can be seen from this figure that there is a linear increase of all these parameters when the PMMA amount is increased in the PVDF/PMMA blends. This indicates the increase of charge transfer between the functional group of the PVDF and PMMA macromolecules, and as a result of this fact, there is an increase of electronic disorder within the optical bandgap. This finding suggests the suitability of these polymeric blends to be used as dispersive parameters controllable optical materials in the design of some advanced optoelectronic devices.

### 3.10. Non-linear optical parameters

Characterization of non-linear optical parameters of an optical material is interesting to identify the

Table 2 — Values of single oscillator energy $E_o$, dispersive energy $E_d$, static refractive index $n_o$, linear optical susceptibility $\chi^{(1)}$, third-order non-linear optical susceptibility $\chi^{(3)}$, and non-linear refractive index $n_2$ of the different composition PVDF/PMMA blend films

| PVDF/PMMA films (wt/wt%) | $E_o$ (eV) | $E_d$ (eV) | $n_o$ | $\chi^{(1)}$ | $\chi^{(3)} \times 10^{14}$ | $n_2 \times 10^{12}$ |
|---|---|---|---|---|---|---|
| 100/0 | 7.9 | 30.0 | 2.18 | 0.30 | 138.0 | 23.9 |
| 80/20 | 6.0 | 12.0 | 1.73 | 0.16 | 11.2 | 2.4 |
| 60/40 | 6.3 | 14.2 | 1.80 | 0.17 | 17.5 | 3.7 |
| 40/60 | 7.5 | 18.0 | 1.84 | 0.19 | 22.3 | 4.6 |
| 20/80 | 7.9 | 22.7 | 1.97 | 0.23 | 48.0 | 9.2 |
| 0/100 | 12.0 | 23.3 | 1.71 | 0.15 | 9.5 | 2.1 |

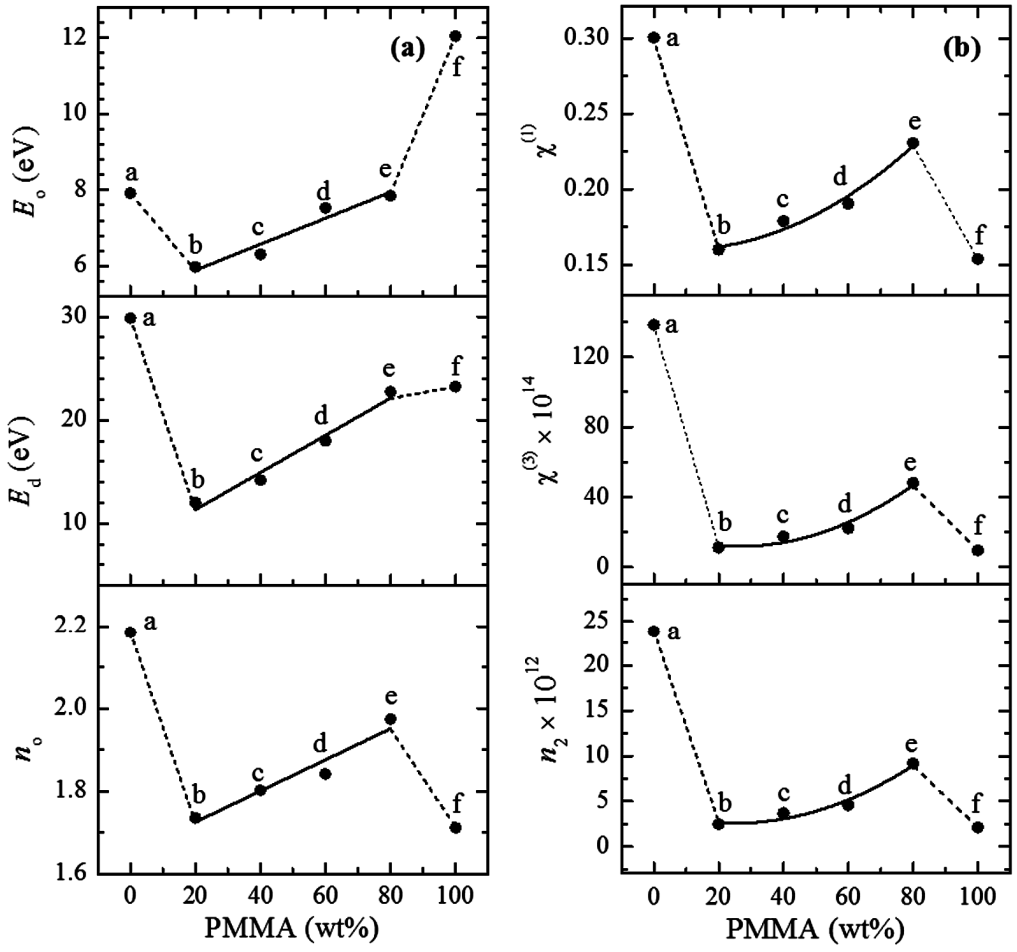


Fig. 8 — Plots of (a) $n_o$, $E_d$, and $E_o$, and (b) $n_2$, $\chi^{(3)}$ and $\chi^{(1)}$ versus PMMA (wt%) for the different compositions PVDF/PMMA blend films. Solid lines in (a) represent the linear fit of the blends data, and in (b) polynomial fit of the blends data.

suitability of such material in the development of advanced non-linear optoelectronic devices. With this fact, the PVDF/PMMA films are characterized for some of the important non-linear parameters. Initially, the value of linear susceptibility $\chi^{(1)}$, and then the values of third-order non-linear susceptibility $\chi^{(3)}$ and non-linear refractive index $n_2$ were computed, respectively using the dispersive parameters ($E_o$, $E_d$, and $n_o$) based relations[27,28,31,36,45] given below as Eqs (13), (14), and (15);

$$\chi^{(1)} = \frac{E_d}{4\pi E_o} \quad \text{... (13)}$$

$$\chi^{(3)} = 6.82 \times 10^{-15} \left( \frac{E_d}{E_o} \right)^4 \quad \text{... (14)}$$

And, $$n_2 = \frac{12\pi\chi^{(3)}}{n_o} \quad \text{... (15)}$$

The computed values of $\chi^{(1)}$, $\chi^{(3)}$, and $n_2$ for the PVDF/PMMA blend films are recorded in Table 2 and also plotted against PMMA (wt%) concentration in Fig. 8(b). It is found that all these non-linear parameters are high for pristine PVDF film as compared to that of the pristine PMMA film (see Table 2). Besides this fact, the $\chi^{(1)}$, $\chi^{(3)}$, and $n_2$ values of the PVDF/PMMA blend films increase non-linearly when the PMMA amount in the blend was increased from 20 wt% to 80 wt% (Fig. 8(b)). The polymer composition-dependent values of $\chi^{(1)}$, $\chi^{(3)}$, and $n_2$ of the PVDF/PMMA blend films also realize these blends appropriateness in the advances of next-generation non-linear optoelectronic devices.

## 4 Conclusion

This paper reports a detailed study on optical behaviour and various optical parameters of the PVDF/PMMA blend films over the entire blend composition range. The absorbance, transmittance, and reflectance spectra of the PVDF/PMMA films in the UV-Vis wavelength range from 200 nm to 800 nm were performed and analyzed for the optical characterization of these materials. These spectra were used for the determination of various optical parameters of the PVDF/PMMA blend films and their dependency on the blend composition was examined. It is explored that the absorbance, reflectance, and transmittance behaviour of these polymer blend films can be controlled especially in the visible photons wavelength range by adjusting the composition of the constituents. The direct energy band gap $E_{gd}$ of the PVDF/PMMA films decreased with the increase of PMMA amount in the blends. The extinction coefficient and refractive index of these polymers blends were also found composition dependent. The optical range dielectric constant of the blend films showed anomalous variation with the alteration in constituent composition but they are characterized as low dielectric loss materials. The optical conductivity of these PVDF/PMMA blends was found in between that of the constituents conductivities. Values of dispersive and non-linear optical parameters of the PVDF/PMMA films were found predominantly dependent on the constituent compositions. This study on the optical behaviour of the PVDF/PMMA blend films and their composition dependence optical parameters provide a basis for polymer blending and design guidance. With the help of these optical parameters, the selection of an appropriate polymer blend composition matrix can be made and used in the design and development of next-generation advanced optoelectronic devices.

## Acknowledgments

The University Grants Commission, New Delhi, is gratefully acknowledged for the experimental grant through SAP DRS-II Project (No. F.530/12/DRS-II/2016(SAP-I)).

## References

1 Aid S, Eddhahak A, Khelladi S, Ortega Z, Chaabani S, & Tcharkhtchi A, *Polym Test*, 73 (2019) 222.
2 Veitmann M, Chapron D, Bizet S, Devisme S, Guilment J, Royaud I, Poncot M, & Bourson P, *Polym Test,* 48 (2015) 120.
3 Zhang Y, Zuo M, Song Y, Yan X, & Zheng Q, *Compos Sci Technol,* 106 (2015) 39.
4 Choudhary S, Dhatarwal P, & Sengwa R J, *Indian J Eng Mater Sci,* 24 (2017) 123.
5 Dhatarwal P, Sengwa R J, & Choudhary S, *Optik,* 221 (2020) 165368.
6 Mohammed M I, *J Mol Struct,* 1169 (2018) 9.
7 Liu Y, Gao J, Yao R, Zhang Y, Zhao T, Tang C, & Zhong L, *Mater Chem Phys,* 250 (2020) 123155.
8 Leppe-Nerey J R, Sierra-Espinosa F Z, Nicho M E, & Basurto-Pensado M A, *Sens Actuators A: Phys,* 317 (2021) 112461.
9 Ali U, Karim K J B A, & Buang N A, *Polym Rev,* 55 (2015) 678.
10 Freire E, Bianchi O, Monteiro E E C, Nunes R C R, & Forte M C, *Mater Sci Eng C,* 29 (2009) 657.
11 Martins P, Lopes A C, & Lanceros-Mendez S, *Prog Polym Sci,* 39 (2014) 683.
12 Ismail A M, Mohammed M I, & Fouad S S, *J Mol Struct,* 1170 (2018) 51.
13 Fan B, Zhou M, Zhang C, He D, & Bai J, *Prog Polym Sci,* 97 (2019) 101143.

14 Bae J H, & Chang S H, *Funct Compos Struct,* 1 (2019) 012003.

15 Lu L, Ding W, Liu J, & Yang B, *Nano Energy,* 78 (2020) 105251.

16 Sengwa R J, & Dhatarwal P, *Opt Mater,* 113 (2021) 110837.

17 AlAbdulaal T H, & Yahia I S, *Optik,* 227 (2021) 166036.

18 Dhatarwal P, Choudhary S, & Sengwa R J, *J Polym Res,* 28 (2021) 63.

19 Dhatarwal P, & Sengwa R J, *Funct Compos Struct,* 3 (2021) 025008.

20 Botsi S, Tsamis C, Chatzichristidi M, Papageorgiou G, & Makarona E, *Nano-Struct Nano-Objects,* 17 (2019) 7.

21 De Souza Leão R, De Moraes S L D, De Luna Gomes J M, Lemos C A A, Da Silva Casado B G, Do Egito Vasconcelos B C, & Pellizzer E P, *Mater Sci Eng C,* 106 (2020) 110292.

22 Gaabour L H, *Opt Photon J,* 10 (2020) 197.

23 Abd El-kader F H, Hakeem N A, Hafez R S, & Ismail A M, *J Inorg Organomet Polym Mater,* 28 (2018) 1037.

24 Zhao X, Chen S, Zhang J, Zhang W, & Wang X, *J Cryst Growth,* 328 (2011) 74.

25 Pawde S M, & Deshmukh K, *J Appl Polym Sci,* 114 (2009) 2169.

26 Li M, Stingelin N, Michels J J, Spijkman M -J, Asadi K, Feldman K, Blom P W M , & De Leeuw D M, *Macromolecules,* 45 (2012) 7477.

27 Soliman T S, & Vshivkov S A, *J Non Cryst Solids,* 519 (2019) 119452.

28 Soliman T S, Vshivkov S A, & Elkalashy Sh I, *Opt Mater,* 107 (2020) 110037.

29 Bhavsar V, & Tripathi D, *Indian J Pure Appl Phys,* 58 (2020) 795.

30 Dhatarwal P, & Sengwa R J, *Optik,* 241 (2021) 167215.

31 Dhatarwal P, & Sengwa R J, *Phys B Condens Matter,* 613 (2021) 412989.

32 Dhatarwal P, Choudhary S, & Sengwa R J, *Indian J Chem Technol* 28 (2021) 693.

33 Khairy Y, Mohammed M I, Elsaeedy H I, & Yahia I S, *Optik,* 212 (2020) 164687.

34 Alsaad A M, Ahmad A A, Al Dairy A R, Al-anbar A S, & Al-Bataineh Q M, *Results Phys,* 19 (2020) 103463.

35 Mohamed M B, & Abdel-kader M H, *Appl Phys A,* 125 (2019) 209.

36 Nafee S S, Hamdalla T A, & Darwish A A A, *Opt Laser Technol,* 129 (2020) 106282.

37 Badawi A, Alharthi S S, Mostafa N Y, Althobaiti M G, & Altalhi T, *Appl Phys A,* 125 (2019) 858.

38 El-Sayed S, Farag Z R, & Saber S, *AIP Adv,* 10 (2020) 095127.

39 Sengwa R J, Choudhary S, & Dhatarwal P, *J Mater Sci: Mater Electron,* 30 (2019) 12275.

40 Sengwa R J, & Dhatarwal P, *J Mater Sci Mater Electron,* 32 (2021) 9661.

41 Dhatarwal P, & Sengwa R J, *Compos Interfaces,* 28 (2021) 827.

42 Choudhary S, & Sengwa R J, *Curr Appl Phys,* 18 (2018) 1041.

43 Wemple S H , & DiDomenico Jr M, *Phys Rev B,* 3 (1971) 1338.

44 Taha T A, *Polym Bull,* 76 (2019) 903.

45 AlAbdulaal T H, & Yahia I S, *Phys B Condens Matter,* 601 (2021) 412628.